Fall 2015

3D Geometric Morphometrics In Modern And Extinct Foot-Propelled Diving Birds: An Evaluation Of The Tarsometatarsus For Species Identification

Mackenzie E. Kirchner-Smith
Fort Hays State University, makirchn@berkeley.edu

3D GEOMETRIC MORPHOMETRICS IN MODERN AND EXTINCT FOOT-PROPELLED DIVING BIRDS: AN EVALUATION OF THE TARSOMETATARSUS FOR SPECIES IDENTIFICATION

being

A Thesis Presented to the Graduate Faculty

of the Fort Hays State University in

Partial Fulfillment of the Requirements for

the Degree of Master of Science

by

Mackenzie E. Kirchner-Smith

B.S., Indiana University Bloomington

Date _____ Approved _____
Major Professor

Approved _____
Chair, Graduate Council

ABSTRACT

Hesperornithiformes (Aves: Ornithurae) were flightless foot-propelled diving birds that lived during the Late Cretaceous and have a good fossil record compared to most Mesozoic birds. Extinct taxa are often identified using fragmentary or isolated specimens, and several species of *Hesperornis* have been named from the morphology of the tarsometatarsus, often relying on size for taxonomic differentiation. However, little has been done to examine intraspecific variation in this bone and evaluate its use for taxonomic identification.

To test for intraspecific and interspecific variation in the tarsometatarsus of hesperornithiforms, variation in extant members of the foot-propelled diving Gaviidae (loons) and Podicipedidae (grebes) was considered. Loons and grebes are morphologically similar to extinct hesperornithiforms, making them appropriate analogues. Only adult female specimens were chosen for analysis to eliminate the possibility of sexual dimorphism or ontogenetic differences. Landmark-based Geometric Morphometrics was performed on 3D scans of specimens from three species per family, totaling 22 modern specimens. Five species of *Hesperornis* were scanned and analyzed, totaling 13 individuals. Separate analyses were performed on the shape of the full bone, the shape of the distal end, and the shape of the proximal end for each clade (Gaviidae, Podicipedidae, and *Hesperornis*).

In nearly every Principal Component (PC) morphospace analysis of extant and extinct groups, individuals did not group by species, and any grouping that did occur was poorly defined. These results indicate that there is too much intraspecific variation and too little interspecific variation to confidently identify a species using only the

tarsometatarsus in foot-propelled divers. Consequently, fossil hesperornithiform taxa described based on the tarsometatarsus alone may not be valid and require reevaluation.

ACKNOWLEDGEMENTS

I would like to thank everyone who helped and supported me through the course of this thesis, your expertise and patience have been more than I could ever have hoped to receive. I would like to give special thanks to my advisor, Dr. Laura Wilson, for all that she has done to teach, aid, and inspire me. I would also like to thank all of my committee members, Dr. Richard Zakrzewski, Dr. Greg Farley, and Dr. David Polly for their advice and support.

In particular I would like to thank Dr. David Polly for writing code specifically for this project, and the Geological Society of America for providing grant funding to make this study possible. I would also like to thank all of the museums that provided specimen loans and access for this study.

And I would like to thank my parents and all of my friends for their support and for never doubting that I could be where I am today.

TABLE OF CONTENTS

Page

LIST OF TABLES

LIST OF FIGURES

INTRODUCTION

The Hesperornithiformes is a group of extinct flightless seabirds that used foot-propulsion to pursue prey in the epicontinental seas of North America, Europe, and Asia during the Cretaceous. Despite their functional similarities to some groups of extant birds such as loons and grebes, they are a branch of avian phylogeny that went extinct at the end of the Cretaceous (Storer, 1960). Adapted to a flightless and marine lifestyle, hesperornids have significantly less pneumatized bones than volant birds (Gilbert et al., 1981), leading to a better fossil record than most Mesozoic birds. Of these bones, the tarsometatarsus has a particularly high preservation potential because it is composed of fused tarsals and metatarsals, making it an especially dense bone (Husband, 1924). Although researchers frequently use this bone to identify bird taxa (e.g., Williston, 1898; Martin, 1984; Martin and Lim, 2002; Bell and Everhart, 2009; Jadwiszczak and Hospitaleche, 2013), little has been done to examine intra- and interspecific variation in the tarsometatarsus.

The purpose of this study is to test for intra- and interspecific variation in the tarsometatarsus using landmark-based 3D Geometric Morphometrics (GMM), thereby evaluating the use of this bone for species identification. Several species of the Hesperornithiformes have been named using only the tarsometatarsus, including *Hesperornis gracilis*, *H. chowi*, *H. bairdi*, *H. mengeli*, *Baptornis advenus*, *Brodavis americanus*, *B. baileyi*, and *B. mongoliensis.* Some of these species have been named primarily on size differences in this bone. *H. gracilis* (Marsh, 1876) and *Baptornis advenus* (Marsh, 1877) have since been described by more complete material. This

analysis will focus on species of the genus *Hesperornis*, which has the highest number of species and the most abundant material.

Although hesperornithiforms have no living descendants, some extant birds, such as loons and grebes, have morphologically similar tarsometatarsi (Zinoviev, 2011). Consequently, tarsometatarsi of extant species of Gaviidae (loons) and Podicipedidae (grebes) were analyzed for both intra- and interspecific variation using 3D Geometric Morphometrics in the present study. Unlike hesperornids, these extant birds are capable of flight, but like hesperornids their primary form of locomotion uses the hindlimb. By utilizing modern taxa with well-resolved species-level taxonomy, species variation can be accurately assessed and used to reevaluate multiple extinct forms.

Landmark-based GMM is a technique that allows comparison of shape by eliminating the scale, rotation, and translation of objects. To date, the majority of GMM studies examining intraspecific variation have been conducted on mammals (e.g., O'Higgins, 2000; Fadda and Corti, 2001; Lockwood et al., 2002; Figueirido et al., 2009). Additionally, most GMM studies that have been used to identify intraspecific variation in fossil taxa have been focused on cranial and dental morphology rather than postcrania. Other statistical studies have examined the limb elements in non-mammalian groups (e.g., Bonnan et al., 2008; Jadwiszczak and Hospitaleche, 2013), but lack a full geometric morphometric approach. Recently, the tarsometatarsi of the extinct penguin *Palaeeudyptes* was subjected to a Principal Components (PC) analysis, but used size-based measurements rather than landmark-based Geometric Morphometrics to determine species boundaries with this bone (Jadwiszczak and Hospitaleche, 2013). They concluded the tarsometatarsus in *Palaeeudyptes* is highly heterogeneous in size, and therefore size

measurements should not be relied upon for taxonomic classification. Evaluating the presence of species variation in the tarsometatarsus with GMM and PC analysis provides additional information to use in fossil species identification. Additionally, this study will bring into question the validity of some currently recognized species of the Hesperornithiformes and more broadly impact how fossil bird material is used to name and identify species.

MATERIALS AND METHODS

Institutional Abbreviations

FHSM VP: Fort Hays State University Sternberg Museum of Natural History, Hays, KS, USA; **KUVP**: University of Kansas Museum of Vertebrate Paleontology, Lawrence, KS, USA; **USNM**: Smithsonian National Museum of Natural History, Washington, DC, USA; **YPM**: Yale Peabody Museum of Natural History, New Haven, CT, USA; **YPM PU**: Yale Peabody Museum of Natural History, New Haven, CT, USA, Princeton University, Princeton, NJ, USA (Specimens from Princeton University now housed at Yale Peabody Museum).

Materials

Five species of the genus *Hesperornis* were analyzed for both intraspecific and interspecific variation and three modern genera from each of the families Gaviidae (loons) and Podicipedidae (grebes), Table 1. Thirteen fossil specimens representing *H. regalis* (Marsh, 1872), *H. chowi* (Martin and Lim, 2002), *H. bairdi* (Martin and Lim, 2002), *H. gracilis* (Marsh, 1876), and a possible specimen of *H. altus* (Shufeldt, 1915) (YPM PU 17208D) were analyzed. Specimen YPM PU 17208D is labeled in collections as *Hesperornis altus*, but the identification of this specimen is noted in the Peabody collections as unverified. For the sake of this analysis, the name *H. altus* is used. Specimens that were each named from an individual tarsometatarsus in this analysis include *Hesperornis chowi* and *Hesperornis bairdi*. Fossils specimens were generally unaltered and well preserved, with a few having cracks or chips in the shaft of the bone. Specimens YPM PU 17208D and YPM 1679 appear to have been broken and re-glued at

the mid-shaft. In the proximal analysis of the tarsometatarsus, an additional two specimens of *H. gracilis* that only consist of a proximal end were included. Right tarsometatarsi were used for the fossil specimens when available, but the right tarsometatarsus was not always available in the fossil material, and so a reversed left was substituted.

Measurements were taken for three species of Gaviidae: *Gavia immer* (Brunnich, 1764) (n=4), *G. stellata* (Lawrence, 1858) (n=4), and *G. pacifica* (Pontoppidan, 1763) (n=3); and three species of Podicipedidae: *Podiceps grisegena* (Boddaert, 1783) (n=4), *P. cristatus* (Linnaeus, 1758) (n=4), and *P. major* (Boddaert, 1783) (n=3). All modern specimens are housed at the USNM. Larger taxa were chosen to provide a more accurate comparison to the consistently large hesperornithiforms. Additionally, larger size allows for higher quality scans, as tarsometatarsi under 60 mm in length could not be accurately scanned due to small surface area. Only the right tarsometatarsi of adult female specimens (based on USNM records) were used in the modern specimen analysis to avoid sexual dimorphic and ontogenetic factors, thus strengthening the taxonomic signal in the analysis.

Data Collection

Scanning

Scans were collected with a 3D Laser Scanner (NextEngine), which uses an array of lasers to capture a 3D mesh of an object to 0.127 mm accuracy. In this analysis a complete 3D mesh for an individual bone consisted of 48 partial scans, in two different orientations, which are then fused together. A single scan of a bone in this analysis

consisted of fixing the bone to a NextEngine scanner bed called the MultiDrive, which is able to rotate and tilt the object for a more accurate point mesh. For the first scan, the bone was mounted at the proximal end on the MultiDrive bed (Fig. 1, A), which moves in three positions: upward tilt, downward tilt, and horizontal. In each position, the bone is automatically rotated and scanned eight times for a total of 24 partial scans. Because this does not allow for the proximal end of the bone to be scanned, the bone must be repositioned on the scanner bed. For the second scan, the bone was fixed to the MultiDrive bed at mid shaft to scan both the distal and proximal articulation surfaces (Fig. 1, B). Again, 24 partial scans were gathered for the three platform positions.

Once partial scans were captured for each of the two scan orientations (Fig. 1), ScanStudio was used to trim excess material from the incomplete 3D images. These images were then digitally refined by the ScanStudio program using the 'refine' tool so that all pieces of the mesh aligned properly. In some cases, the mesh required manual alignment due to the complexity of the bone surface. In these cases, morphologically corresponding points were placed on each scan to help with alignment. Once each partial scan was trimmed and aligned, a completed scan from each of the two positions was merged into one complete 3D object.

Point Placement

Landmark-based GMM uses points placed on 2D or 3D surfaces to allow for a quantitative comparison of individual shapes (Bookstein et al., 1985). Although 2D analysis gives an accurate depiction of shape change, 3D analyses provide more insight into the overall shape (Meyer et al., 2009). 3D GMM analyses use hundreds or thousands

of points to create a network of landmarks that encompass the entire shape of the object. Points are either landmarks, which are homologous points of correspondence, or semi-landmarks, which are defined by their position on a surface but are able to 'slide' in order to incorporate more information about curved geometry. The Landmark (Wiley et al., 2005) program allows the user to place individual points, as well as patches, on the surface of the bone. Patches consist of a set number of landmark points and semi-landmarks that cover larger areas and more accurately represent curved surfaces. Point patches were used to maximize coverage of the bone surface and major curvatures.

GMM requires all of the elements to align (i.e., all specimens must be from the same side), but mirror images may be used in cases where the only specimen is from the opposite side (Zelditch et al., 1992). The differences between a left and right bone are considered random and are referred to as fluctuating asymmetry, so no error was introduced when a mirrored bone was used in place of a matching side (Van Valen, 1962; Leamy and Klingenberg, 2005). Mirroring is particularly useful for fossil specimens, as they are often incomplete. The majority of the fossil specimens were right tarsometatarsi, so images were mirrored in Landmark before landmark points were placed in cases where only left tarsometatarsi were available for analysis.

Landmark points were placed in the same location on each bone for accurate comparison. Landmark has the capability to semi-automatically place landmark points across a group of scans from a randomly chosen bone in the data set, which is designated as the atlas bone. Points were manually placed along the surface of the chosen atlas bone, and these points were transferred from the atlas to all other bones in the analysis. A minimum of four morphologically corresponding landmarks were placed manually to link

between the atlas and the next bone in the analysis and were the basis for the transfer of all other points. It is semi-automatic, which means that the points are not touching the surface of the bone and must be manually moved to the surface, but the points are already in the appropriate corresponding locations for this placement and require only minor adjustments. This allowed for the placement of a large number of points on many bones relatively quickly.

USNM 500851 was used as the atlas for all *Gavia* specimens, with 893 points placed along the entire bone, including 351 on the distal end and 236 on the proximal end. For *Podiceps*, USNM 612740 was the atlas. Points were modified from USNM 500851, with 896 points placed along the entire bone, including 351 on the distal end and 230 on the proximal end. YPM 1200, the type specimen of *Hesperornis regalis*, was used as the atlas for all fossil bones. Points were modified from USNM 500851, with 960 points placed along the entire bone, including 448 on the distal end and 269 on the proximal end.

Geometric Morphometrics

GMM analyses were performed in Mathematica (Wolfram Research, Inc., 2010). After placing landmark points on each specimen, the points were imported out of Landmark as an individual 3D points file (.pts) for each specimen. PTS files were converted to plain text files (.txt) and imported into nine Excel spreadsheets to group them for analysis. Groupings were all points, distal points, and proximal points for *Gavia*, *Podiceps*, and *Hesperornis*. The Excel sheets were then converted back to plain text files to be readable in Mathematica. The Mathematica code used was written and modified by

Dr. David Polly of Indiana University Bloomington for 2D and 3D morphological shape comparisons (Polly and Goswami, 2010; Polly, 2012, 2013, 2015). Using this code, the plain text files from the Excel spreadsheets were imported into Mathematica and were each subjected to Procrustes superimposition and a PC analysis.

Procrustes superimposition removes aspects of size including rotation, scale, and translation from the objects of the analysis. The Procrustes analysis takes the landmark data collected from all shapes in the analysis and creates an average shape, which lies at the centroid (0,0) of the graph (Bookstein, 1996). The amount of variance that each specimen shows compared to the average shape is calculated and these values are placed on a morphospace, resulting in a PC analysis. The resulting PC morphospace is a graphical representation of shape change in the data set. This analytical function gives a percentage to every change in shape occurring in the set of points, and assigns them to PC1, PC2, PC3, etc. PC1 represents the most significant change in the shape and subsequent PCs are listed in order of decreasing percentage.

In the PC morphospace, every point represents one bone and is placed along the x-axis according to the amount of difference it shows from the centroid x coordinate, and along the y-axis according to the amount of difference it shows from the centroid y coordinate. Each axis of a PC morphospace is representative of a PC. For this analysis, the x-axis is represented by PC1 and the y-axis is represented by PC2, which are the first and second highest areas of shape change, respectively. Individual specimens that are close together on the PC morphospace are more similar in shape to each other than to individuals further away.

Analysis of Variance (ANOVA)

An ANOVA was performed for the PC1 of each graph to statistically determine what percent of PC1 is explained by species and which species groups are significantly different from each other, should a difference be present. An ANOVA test analyzes the variance of the means between two or more groups, and produces a p-value indicating whether or not the results are statistically significant, and an R^2 value indicating what percentage of the overall variation is species variation. If the p-value is 0.05 or higher, variation among groups is likely caused by chance and indicates low interspecific variation. If the p-value is below 0.05, this indicates there is some variation among the groups that is not caused by chance. If the p-value is below 0.05, the R^2 value then indicates the percentage of variation of PC1 that is explained by species. Multiplying this number by the PC1 percentage gives the percentage of variation on PC1 that is accounted for by species. A Bonferroni correction will distinguish which species are significantly different from each other, if any differences are present.

RESULTS

Gavia Tests

The initial full bone shape analysis of the *Gavia* specimens shows a very loose grouping by species, with PC1 accounting for 38.99% of the shape change in the bone and PC2 accounting for 17.61% (Fig. 3 A). Increasing along the x-axis of the PC morphospace (PC1), the hypotarsal ridge at the proximal end changes from a flatter to a more rounded edge (Fig. 3 B), but some individuals of *G. stellata* have an edge more similar to that of *G. pacifica* individuals than to individuals of their own species. For example, USNM 500337 is closer on both the x- and y-axis to USNM 491640 than it is to one of its own species, USNM 489530. As shape change increases along the PC2 axis, the articular surface of the second trochlea becomes wider and the groove of this surface more pronounced (Fig. 3 C).

The proximal shape analysis yields no taxonomic groupings and slightly less overall variability than the full bone analysis (Fig. 4 A). All three species overlap in the morphospace, with individuals of different species falling closer to each other than to their own species. PC1 accounts for 24.59% of the total shape change in the proximal end of the tarsometatarsus if *Gavia*, and reflects change along the hypotarsal ridge (Fig. 4 C, E); this ridge becoming more pronounced and pointed increasing along the x-axis. PC2 accounts for 22.18% of the total shape change and reflects the region where the hypotarsal ridge connects to the ventral side of the bone shaft (Fig. 4 C). The curve of this ridge as it connects to the bone shaft also becomes deeper moving up the y-axis of the morphospace (Fig. 4 D).

The distal shape analysis (Fig. 5 A) yields slightly higher variability than the proximal, but still less than the full bone analysis (Fig. 4 A). Similar to the proximal test, all three *Gavia* species exhibit significant overlap with no distinct taxonomic grouping. In the distal end of the *Gavia* tarsometatarsus, PC1 accounts for 30.60% of the total variation and is caused by an increase in width of the tendinal canal (Fig. 5 B). PC2 accounts for 23.68% of the total variation and is focused on the medial edge of the third trochlea, which becomes rounder in medial view as variation increases along the y-axis (Fig. 5 E).

The difference among the *Gavia* species is due to more than random chance in the shape of the full bone as indicated by an ANOVA p-value of 0.003 (Table 2). A Bonferroni correction indicates that *G. immer* is significantly different from both *G. pacifica* and *G. stellata*, but that the latter two species do not significantly differ from each other. Approximately 29.80% of the total variation in PC1 can be attributed to species differences. An ANOVA for the proximal shape of *Gavia* results in a p-value of 0.035. The proximal end of *G. immer* differs significantly from *G. stellata*, but no other significant difference is found. 13.95% of the variation of PC1 is explained by species differences (Table 2). An ANOVA of the distal end resulted in a p-value that is not below 0.05.

Podiceps Tests

The full bone analysis of *Podiceps* is very similar to *Gavia*, with significant overlap between all three species and little overall variation in the tarsometatarsus (Fig. 6 A). The most significant shape change in this analysis is concentrated at the proximal end

of the tarsometatarsus (Fig. 6 B-E). PC1 accounts for 44.17% of the total variation, and changes as the right ridge around the proximal foramina becomes more pronounced and triangular, extending down the shaft of the bone to approximately the middle of the shaft (Fig. 6 D). PC2 explains 20.88% of the total variation and represents the increase in length and width of the hypotarsal ridges in relation to the length of the bone, with the change being greater in the left hypotarsal ridge (Figure 6 C). A minimal amount of shape change occurs in the second trochlea of the distal end (Fig. 6 C, E), but not enough to account for PC1 or PC2.

Despite a higher level of variation and morphospace separation of specimens in the proximal end of the tarsometatarsus of *Podiceps*, no groupings of the three species is evident (Fig. 7 A). *P. cristatus* and *P. grisegena*, in particular, overlap to a large degree in the morphospace and group together. In this analysis, most of the variation is in the ridges around the proximal foramina. PC1 accounts for 48.22% of the total variation and is defined by the increase of depth in the right proximal foraminal ridge (Fig. 7 B, E). PC2 accounts for 13.14%, with shape change focused on the depth of the curve of the left ridge of the proximal foramina as it meets the shaft of the bone (Fig. 7 B, D).

Analysis of the distal end of the tarsometatarsus of *Podiceps* indicates very similar results to the full bone analysis of this group, with little overall variation and no taxonomic differentiation (Fig. 8 A). Individuals of all species plot closely with each other. Shape change in the distal end is focused around the dorsal groove made by the dorsoplantar foramen (PC1) and the articulation surface of the second trochlea (PC2) (Fig. 8 C). PC1 represents 36.67% of the shape change, with an increase along the morphospace x-axis representing the dorsal opening of the dorsoplantar foramen moving

closer to the trochlea (Fig. 8 C). PC2 represents 13.87% of the distal shape variation, which focuses on the proximal portion of the second trochlea articular surface. Increasing along the y-axis of the morphospace, this portion of the trochlea becomes less rounded, with additional bone material connecting it to the shaft (Fig. 8 C, E).

An ANOVA of the full bone analysis of *Podiceps* results in a p-value below 0.05, but a Bonferroni correction indicates that none of the species are significantly different from each other. Distal and proximal tests on *Podiceps* do not have p-values below 0.05 (Table 2).

Hesperornis Tests

Tests on the full tarsometatarsus of *Hesperornis* indicate there is very little overall variation in the shape of this bone (Fig. 9 A), even in specimens identified as different species (Table 1). Variation in the full bone is primarily located in PC1 on the second trochlea of the distal end, accounting for 40.78% of the variation (Fig. 9 B). The most distal end of the second trochlea shifts inward towards the third trochlea with increasing values along the morphospace x-axis (Fig. 9 B). PC2 accounts for just 13.63% of the variation and represents change in the dorsal region of the mid-shaft. However, many of the specimens share a break or crack in a similar location of the shaft where variation represented by PC2 occurs (Fig. 10), indicating that the shape change is focusing on this feature.

An analysis of the proximal end shows low variation in the overall shape and no species differentiation in the morphospace (Fig. 11 A), with shape change focused in the ridges of the dorsal groove that runs down the length of the bone shaft. PC1 explains

23.05% of the shape-change, with the amount of curvature of the right ridge increasing distally (Fig. 11 B). The shape change represented by PC2 is in a similar location to PC1, but in the left ridge of the dorsal groove. Accounting for 13.88% of the shape change, the left ridge increases in depth along the morphospace y-axis (Fig. 11 B).

The majority of the shape change in the fossil specimens occurs distally, and placement of the specimens in the distal analysis morphospace is similar to those in the full bone analysis (Fig. 12 A). As in the full bone analysis, PC1 (45.29%) accounts for the distal most tip of the second trochlea shifting inward towards the third trochlea (Fig. 12 C). PC2 (17.86%) accounts for the anterior most tip of the second trochlea becoming displaced from the anterior most tip of the third trochlea when viewed laterally, while also becoming more pointed than rounded (Figure 12 E).

ANOVA tests of the full, distal, and proximal analyses of *Hesperornis* all resulted in p-values higher than 0.05, meaning no significant difference was found among these fossil species in any part of the bone (Table 2).

DISCUSSION

The GMM analyses suggest that the tarsometatarsus should not be used for species identification in foot-propelled diving birds. Analyses of loon and grebe tarsometatarsi were performed to support whether or not this bone is appropriate for taxonomic identification. Modern species of birds can be distinguished by plumage, biogeographic range, molecular data, and a number of other means that are often not available for fossil specimens. Fossil specimens are reliant on skeletal morphology, so skeletal metrics need to be tested for species variation when comparing fossil and modern taxa. The results of this study indicate the shape of the tarsometatarsus does not strongly correlate to species. Rather, individuals of different species plot closely together in the morphospace, suggesting that intraspecific variation is greater than interspecific variation in this bone. Even in the full bone analysis of *Gavia*, which was statistically significant, only some of the species are significantly different from each other, rather than all three species being distinctly different.

The literature for Hesperornithiformes apomorphies has many inconsistencies (see Bell and Chiappe, 2015), leading to taxonomic confusion. Additionally, several species of *Hesperornis*, including *H. chowi* and *H. bairdi*, have been named using only a single tarsometatarsus. According to Martin and Lim (2002) the tarsometatarsus of *H. chowi* is approximately the size of *H. regalis*, but with a more slender shaft and less enlarged trochlea than those of *H. regalis*. *H. bairdi* is diagnosed as smaller than *H. gracilis*, and differs from *Parahesperornis* in that trochlea II is enlarged and more distal to trochlea III. However, when the tarsometatarsi *H. chowi* and *H. bairdi* were compared to each other and to *H. regalis* in the morphospace (Figs. 9 A, 11 A, 12 A), these character differences

were not observed and no statistically significant differences were detected to support *H. chowi* and *H. bairdi* as valid species.

Using current *Hesperornis* taxonomy, the specimens included in this analysis demonstrate high intraspecific variation, similar to extant loons and grebes. ANOVA analyses of these specimens show that morphological differences in the tarsometatarsus cannot be attributed to species differences (Table 2). The species *Hesperornis chowi* and *H. bairdi* (Martin and Lim, 2002), which are known only from a right and left tarsometatarsus, respectively, fall very close to one another in the morphospace (Figure 9 A). These specimens also fall very close to specimen YPM 1207, identified as *H. regalis*, which indicates that all three of these specimens have very similar morphologies and the variation that is present is not a result of inherent species differences.

Low variation present in the fossil hesperornid specimens emphasizes the need for a taxonomic revision of Hesperornithiformes named from just the tarsometatarsus. This and other recent studies (Bell, 2013; Bell and Chiappe, 2015) question the validity of the species *Hesperornis chowi* and *Hesperornis bairdi* due to their lack of morphological difference from *Hesperornis regalis*, and the lack of evidence that the tarsometatarsus can be used to identify or name new species. Bell and Chiappe (2015) synonymized several species into *H. regalis*, including *H. chowi* (YPM PU 17208), as they found no morphological differences between this specimen and the type of *H. regalis* (YPM 1200). *H. bairdi* (YPM PU 17208-A) differs from *H. regalis* by the distal end of trochlea IV being only slightly further than trochlea III. Consequently, it is unclear if the smaller size of this specimen is due to ontogeny, other intraspecific variation, or a true phylogenetic difference. Previous studies (e.g., Jadwiszczak and Hospitaleche, 2013) have looked at

the tarsometatarsus and determined that size is not a very reliable species identifier, yet many of these *Hesperornis* specimens (e.g., *H. bairdi*, *H. mengeli*) have been named largely on having a smaller size than other *Hesperornis* species. Regardless, the results of the PC analyses support the Bell and Chiappe (2015) reassignment of *H. chowi* to *H. regalis*.

Although the study presented here was limited to extant individuals of adult female loons and grebes, this approach should not be considered a realistic control when working with fossil specimens where sex and age cannot be determined. However, because specimens were chosen to eliminate sexual or ontogenetic differences, this study can confidently conclude that the differences that are seen among these specimens are related to intraspecific variation rather than interspecific variation. Unfortunately, the tarsometatarsus has never been evaluated for histological determination of age, making it unclear if this bone is a good candidate for ontogenetic study. Without the determination of age, it is difficult to justify assigning a species to specimens based solely on size.

CONCLUSIONS

This study tests for intra- and interspecific variation in the tarsometatarsus of foot-propelled diving birds with implications for the validity of using this bone for species identification. Geometric Morphometrics and the resulting Principal Component analyses reveal higher intraspecific than interspecific variation in all foot-propelled divers included in this study. Using extant specimens allows for the evaluation of the taxonomic signal of the tarsometatarsus at the species level, and analyses reveal too much intraspecific variation and too little interspecific variation to identify species based on the tarsometatarsus alone.

As extant species of foot-propelled divers cannot be identified to the species level using the tarsometatarsus, it cannot be assumed that fossil hesperornids can be named or identified from this bone, either. In fact, based on current identifications, *Hesperornis* species show a similar amount of intraspecific variation to the modern specimens. Specimens identified as *H. regalis* show large amounts of intraspecific variation and *H. gracilis* specimens plot with each other, but also lot nearly on top of the type specimen of *H. regalis*. These results show that there is very little difference in the morphology of these individual bones and they cannot be used for identification to species level in either extant or extinct foot-propelled diving birds.

This study provides statistical support for the reassignment of *Hesperornis chowi* to *H. regalis* as proposed by Bell and Chiappe (2015). In addition, *H. bairdi* was very similar to *H. regalis* and should likely be considered a tentative species at best. Other specimens in the Hesperornithiformes that have been assigned to new species using the

tarsometatarsus, such as *H. mengeli*, *Brodavis americanus*, *B. baileyi*, and *B. mongoliensis,* warrant further investigation and reevaluation.

In future work, this analysis will be expanded to include male and juvenile specimens to examine the possibility of sexual dimorphism and ontogenetic variation in the tarsometatarsal shape. Additionally, larger sample sizes of modern specimens will be utilized in order to strengthen the statistical significance of these findings.

LITERATURE CITED

Bell, A., and M. J. Everhart. 2009. A new specimen of *Parahesperornis* (Aves: Hesperornithiformes) from the Smoky Hill Chalk (Early Campanian) of western Kansas. Transactions of the Kansas Academy of Science 112:7–14.

Bell, A., and L. M. Chiappe. 2015. A species-level phylogeny of the Cretaceous Hesperornithiformes (Aves: Ornithuromorpha): implications for body size evolution amongst the earliest diving birds. Journal of Systematic Palaeontology 1–13.

Bell, A. K. 2013. Evolution & ecology of Mesozoic birds: a case study of the derived Hesperornithiformes and the use of morphometric data in quantifying avian paleoecology. University of Southern California. Unpublished dissertation.

Bonnan, M. F., J. O. Farlow, and S. L. Masters. 2008. Using linear and geometric morphometrics to detect intraspecific variability and sexual dimorphism in femoral shape in *Alligator mississippiensis* and its implications for sexing fossil archosaurs. Journal of Vertebrate Paleontology 28:422–431.

Bookstein, F. L. 1996. Combining the tools of geometric morphometrics; pp. 131–151 in Advances in Morphometrics. L.F. Marcus, M. Corti, A. Loy, G. Naylor, and D. Slice (eds.) Plenum Press, New York.

Bookstein, F. L., B. Chernoff, R. L. Elder, J. M. Humphries, G. R. Smith, and R. E. Strauss. 1985. Morphometrics in evolutionary biology: the geometry of size and shape change, with examples from fishes. Philadelphia, PA. Academy of Natural Sciences 277.

Fadda, C., and M. Corti. 2001. Three-dimensional geometric morphometrics of *Arvicanthis*: implications for systematics and taxonomy. Journal of Zoological Systematics and Evolutionary Research 39:235–245.

Figueirido, B., P. Palmqvist, and J. A. Pérez-Claros. 2009. Ecomorphological correlates of craniodental variation in bears and paleobiological implications for extinct taxa: an approach based on geometric morphometrics. Journal of Zoology 277:70–80.

Gilbert, B. M., L. D. Martin, and H. G. Savage. 1981. Avian Osteology. Bone Books, Published by B. M. Gilbert, p. 11.

Jadwiszczak, P., and C. Hospitaleche. 2013. Distinguishing between two Antarctic species of Eocene *Palaeeudyptes* penguins: a statistical approach using tarsometatarsi. Polish Polar Research 34:237–252.

Leamy, L. J., and C. P. Klingenberg. 2005. The genetics and evolution of fluctuating asymmetry. Annual Review of Ecology, Evolution, and Systematics 1–21.

Lockwood, C. A., J. M. Lynch, and W. H. Kimbel. 2002. Quantifying temporal bone morphology of great apes and humans: an approach using geometric morphometrics. Journal of Anatomy 201:447–464.

Marsh, O. C. 1876. Notice of new Odontornithes. American Journal of Science 509–511.

Marsh, O. C. 1877. Characters of the Odontornithes, with notice of a new allied genus. American Journal of Science 79:85–87.

Martin, L. D. and J. -D. Lim. 2002. New Information on the Hesperornithiform Radiation. Proceedings of the 5th Symposium of the Society of Avian Paleontology and Evolution 165–174.

Martin, L. D. 1984. A New Hesperornithid and the relationships of the Mesozoic birds. Transactions of the Kansas Academy of Science 87:141–150.

Meyer, M. G., M. Fauver, J. R. Rahn, T. Neumann, F. W. Patten, E. J. Seibel, and A. C. Nelson. 2009. Automated cell analysis in 2D and 3D: A comparative study. Pattern Recognition 42:141–146.

O'Higgins, P. 2000. The study of morphological variation in the hominid fossil record: biology, landmarks and geometry. Journal of Anatomy 197:103–120.

Polly, P. D. 2012. Quantitative Paleontology for Mathematica. Department of Geology, Indiana University: Bloomington, Indiana.

Polly, P. D. 2013. Geometric Morphometrics for Mathematica. Department of Geology, Indiana University: Bloomington, Indiana.

Polly, P. D. 2015. Zie Morphometrics for Mathematica. Department of Geology, Indiana University: Bloomington, Indiana.

Polly, P. D., and A. Goswami. 2010. Modularity for Mathematica. Department of Geological Sciences, Indiana University: Bloomington, Indiana.

Storer, R. W. 1960. Evolution in the diving birds. Proceedings of the XII International Ornithological Congress 2:694–707.

Van Valen, L. 1962. A study of fluctuating asymmetry. Evolution 125–142.

Warheit, K. I. 1992. The role of norphometrics and cladistics in the taxonomy of fossils: a paleornithological example. Systematic Biology 41:345–369.

Williston, S. W. 1898. Birds. The University Geological Survey of Kansas, Paleontology 4:43–49.

Wolfram Research, Inc. 2010. Mathematica. Champaign, IL.

Zelditch, M. L., F. L. Bookstein, and B. L. Lundrigan. 1992. Ontogeny of integrated skull growth in the cotton rat *Sigmodon fulviventer*. Evolution 1164–1180.

Zinoviev, A. V. 2011. Notes on the hindlimb myology and syndesmology of the Mesozoic toothed bird *Hesperornis regalis* (Aves: Hesperornithiformes). Journal of Systematic Palaeontology 9:65–84.

TABLES AND FIGURES

Table 1. Modern and fossil specimen ID numbers and tarsometatarsal length.

Modern Specimens			
Genus	**Species**	**Institution ID #**	**Length (mm)**
Gavia	*immer*	USNM 500851	80.24
		USNM 501589	89.55
		USNM 501590	84.05
		USNM 501594	82.79
	pacifica	USNM 489530	73.08
		USNM 492476	70.32
		USNM 500337	69.56
	stellata	USNM 491640	72.27
		USNM 556288	73.32
		USNM 560117	71.78
		USNM 561072	73.42
Podiceps	*cristatus*	USNM 554120	61.35
		USNM 557532	60.27
		USNM 560594	68.87
		USNM 560596	60.50
	grisegena	USNM 612740	60.12
		USNM 612741	65.95
		USNM 612744	62.06
		USNM 612747	61.09
	major	USNM 227344	61.64
		USNM 343090	68.56
		USNM 614513	64.64
Fossil Specimens			
Genus	**Species**	**Institution ID #**	**Length (mm)**
Hesperornis	*altus* (?)	YPM PU 17208D	131.90
	bairdi	YPM PU 17208A	102.89
	chowi	YPM PU 17208	137.79
	gracilis	YPM 1473	
		YPM 1478	137.82
		YPM 1679	127.38
		YPM 55000 (Cast)	123.19
		KUVP - No #	
	regalis	YPM 1200	136.28
		YPM 1207	137.20
		YPM 1476	136.85
		FHSM VP 2069	131.00
		KU VP 71012	129.59

Table 2. ANOVA test results for PC1, with * denoting a significant p-value of < 0.05.

Test		PC1 (%)	p-value	R^2	Species Variation (%)
Gavia	Full	38.99	0.003*	0.764	29.80
	Proximal	24.59	0.035*	0.567	13.95
	Distal	30.60	0.961	0.009	0.298
Podiceps	Full	44.17	0.036*	0.564	24.91
	Proximal	48.22	0.088	0.455	21.95
	Distal	36.67	0.113	0.421	15.42
Hesperornis	Full	40.78	0.996	0.038	1.55
	Proximal	23.05	0.769	0.184	4.25
	Distal	45.29	0.976	0.066	2.97

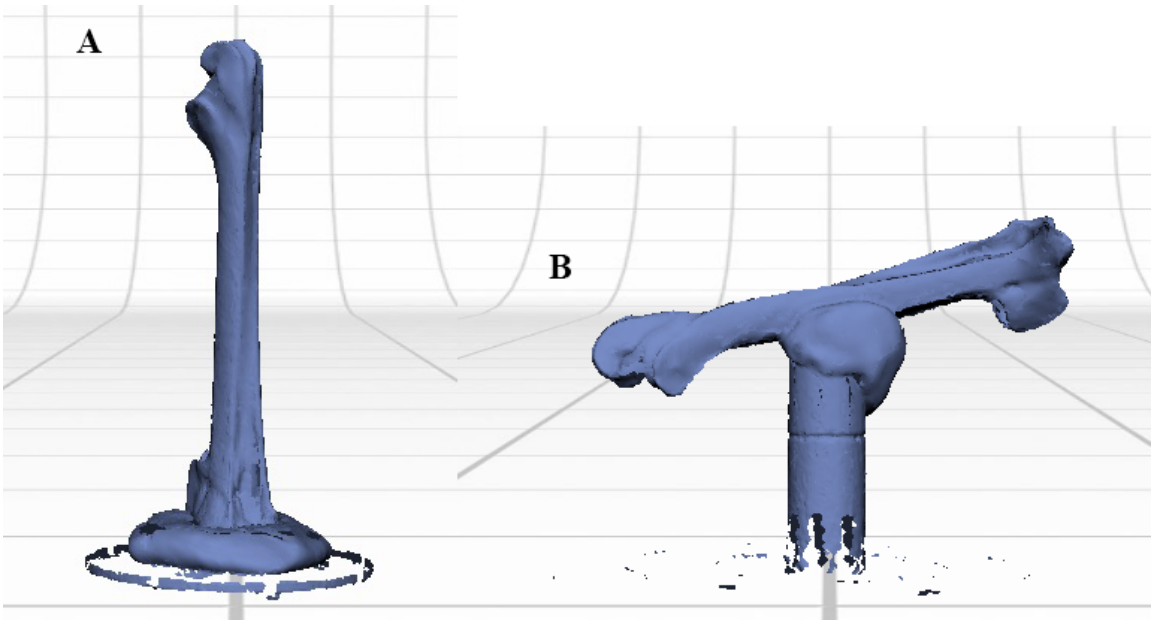

Figure 1: Unedited 3D renderings of a single tarsometatarsus of a loon, showing the positions of the bones during the first (A) and second (B) scan. Initial scan is mounted at proximal base to the scanner bed (A) and the second scan is mounted at mid-shaft (B) to fill in missing surface area.

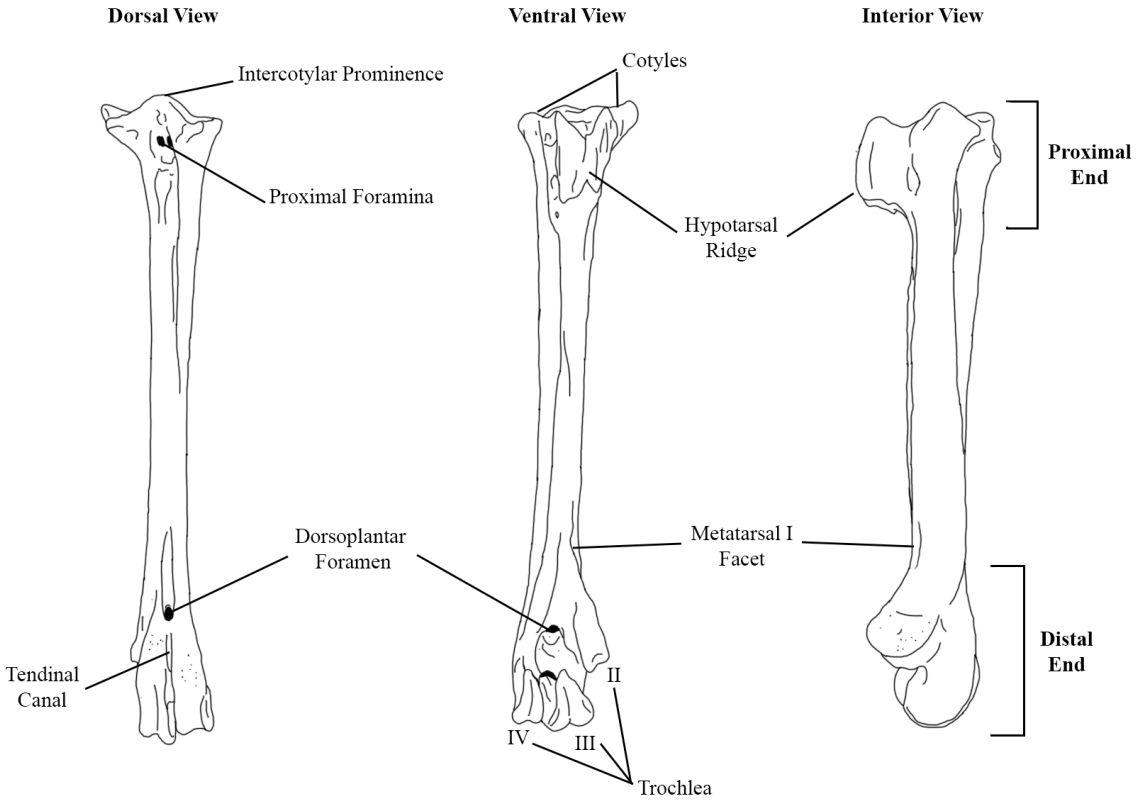

Figure 2: Left tarsometatarsus of *Gavia immer*, the Great Northern Loon.

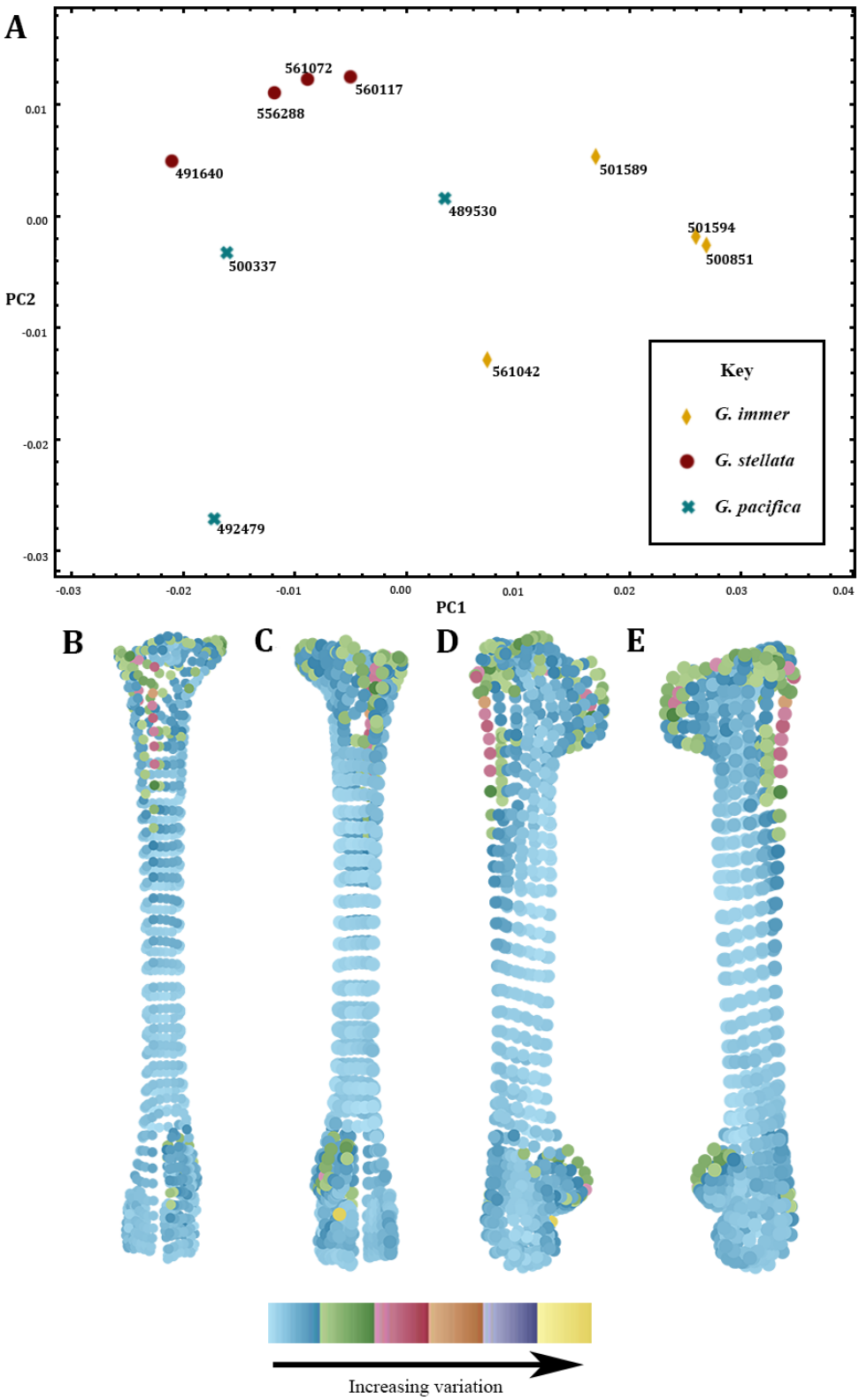

Figure 3: A) PC morphospace showing shape analysis for the full tarsometatarsus of *Gavia immer*, *G. stellata*, and *G. pacifica*. B) Dorsal view of variation map, C) ventral view, D) interior view, E) exterior view.

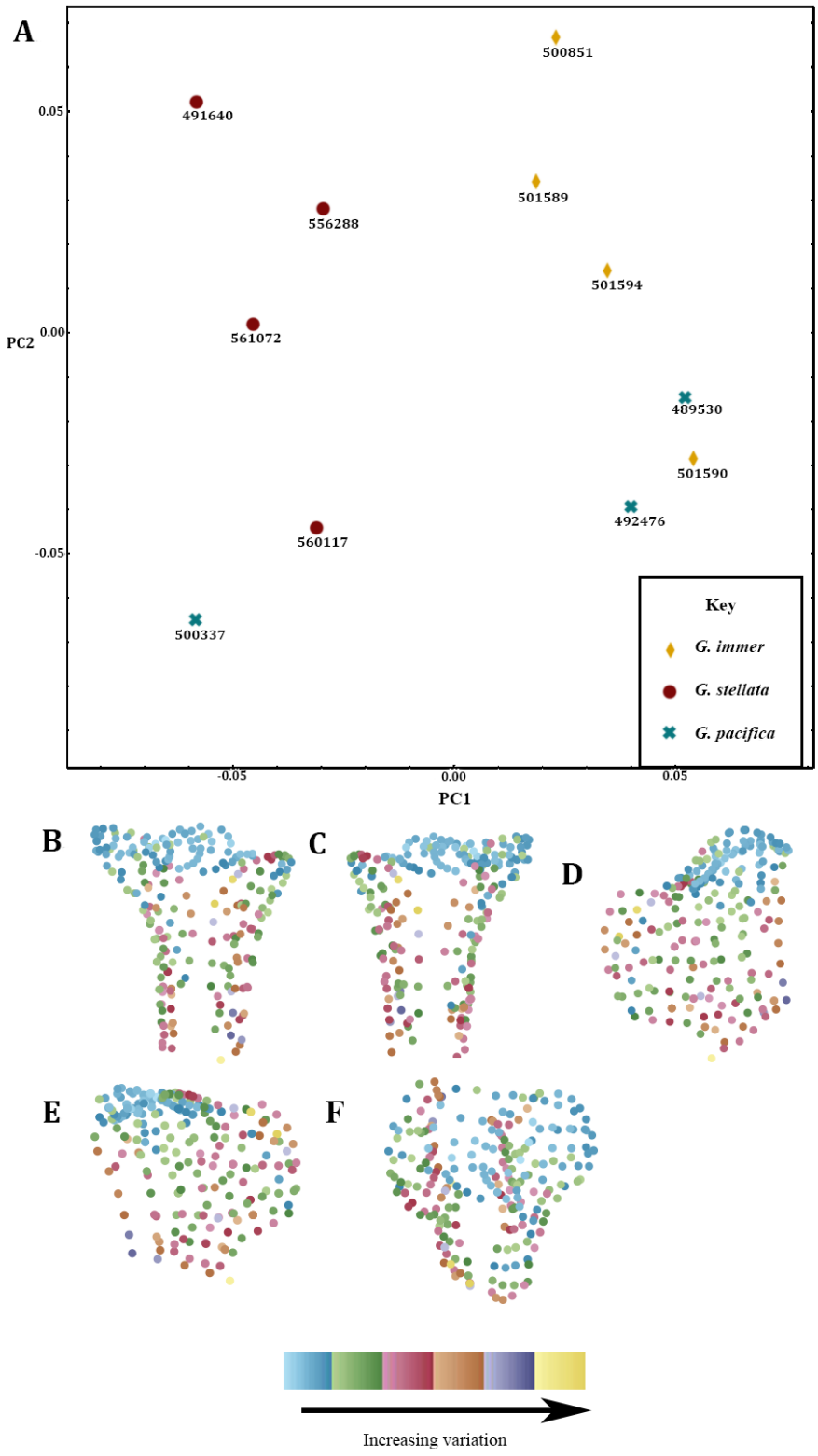

Figure 4: A) PC morphospace showing shape analysis for the proximal tarsometatarsus of *Gavia immer*, *G. stellata*, and *G. pacifica*. B) Dorsal view of variation map, C) ventral view, D) interior view, E) exterior view, F) proximal view.

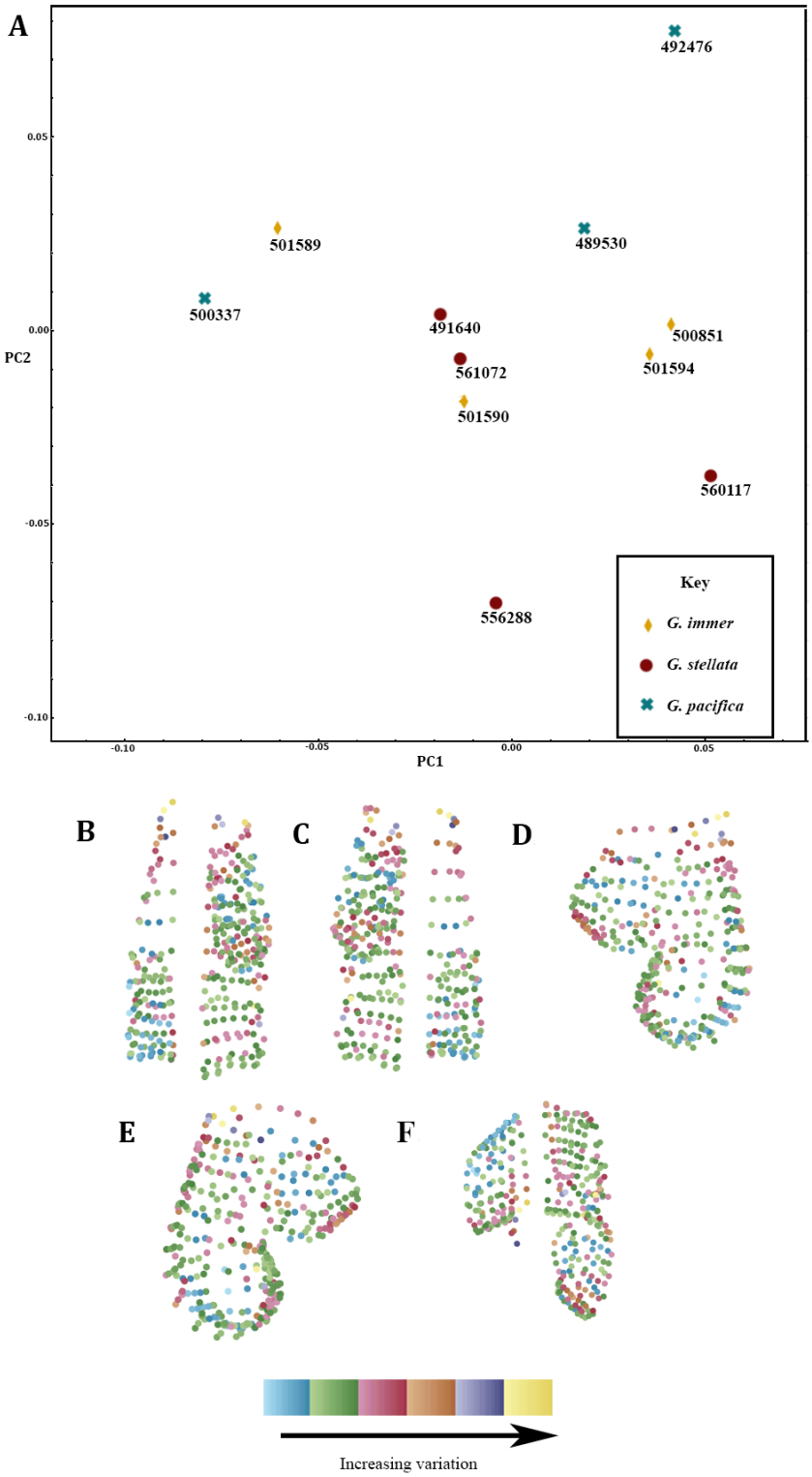

Figure 5: A) PC morphospace showing shape analysis for the distal tarsometatarsus of *Gavia immer*, *G. stellata*, and *G. pacifica*. B) Dorsal view of variation map, C) ventral view, D) interior view, E) exterior view, F) distal view.

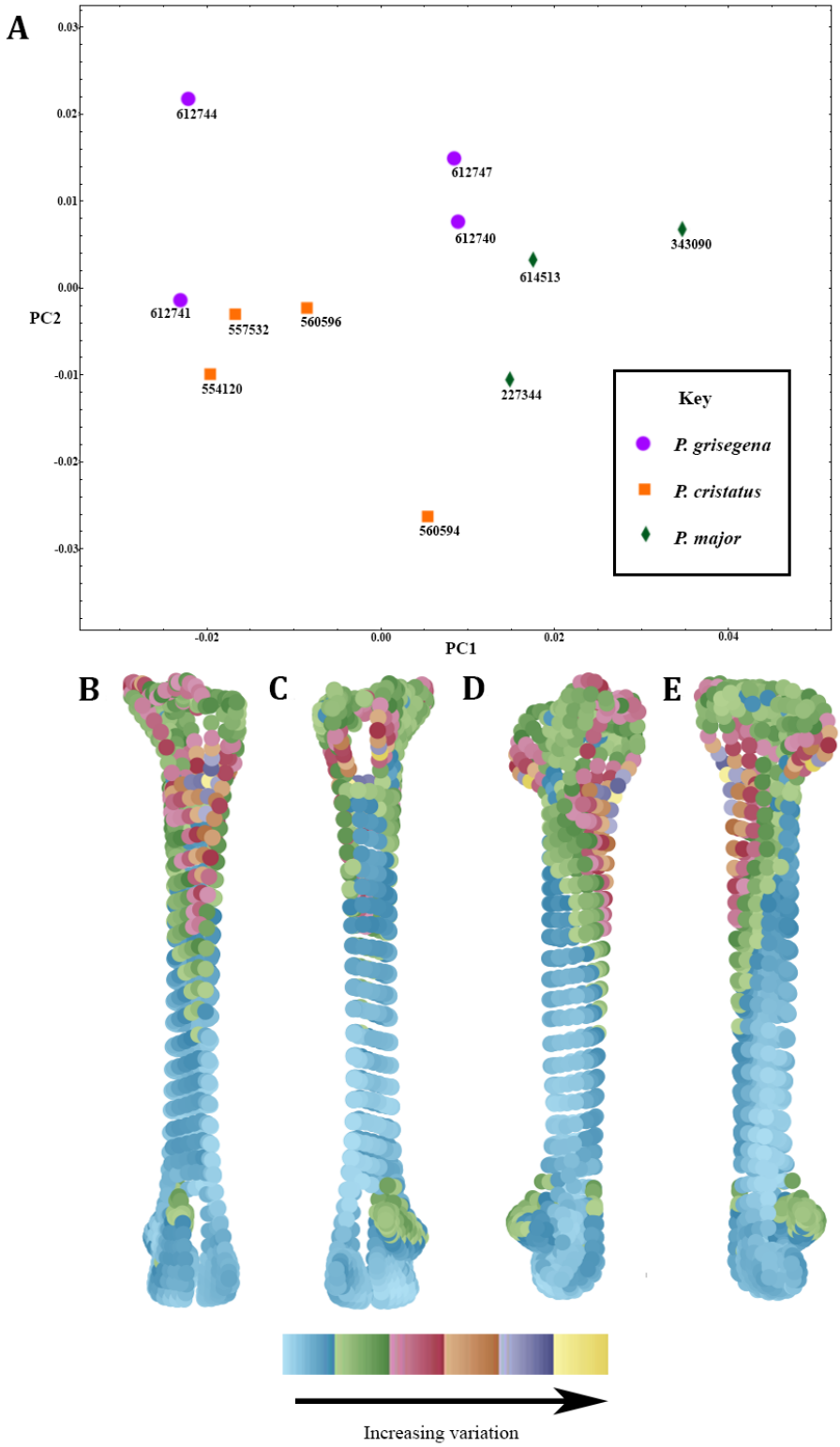

Figure 6: A) PC morphospace showing shape analysis for the full tarsometatarsus of *Podiceps grisegena*, *P. cristatus*, and *P. major*. B) Dorsal view of variation map, C) ventral view, D) exterior view, E) interior view.

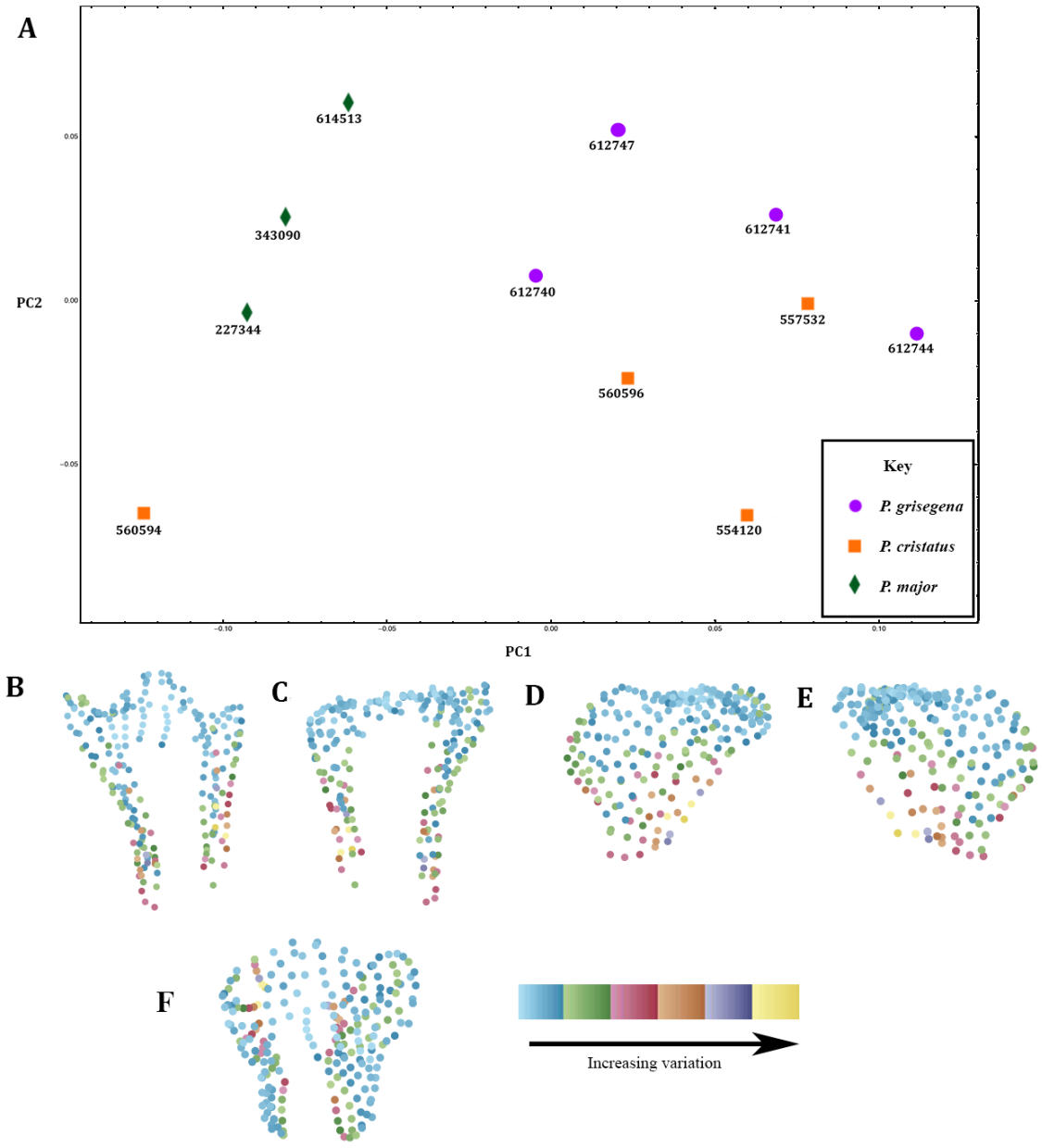

Figure 7: A) PC morphospace showing shape analysis for the proximal tarsometatarsus of *Podiceps grisegena*, *P. cristatus*, and *P. major*. B) Dorsal view of variation map, C) ventral view, D) exterior view, E) interior view, F) proximal view.

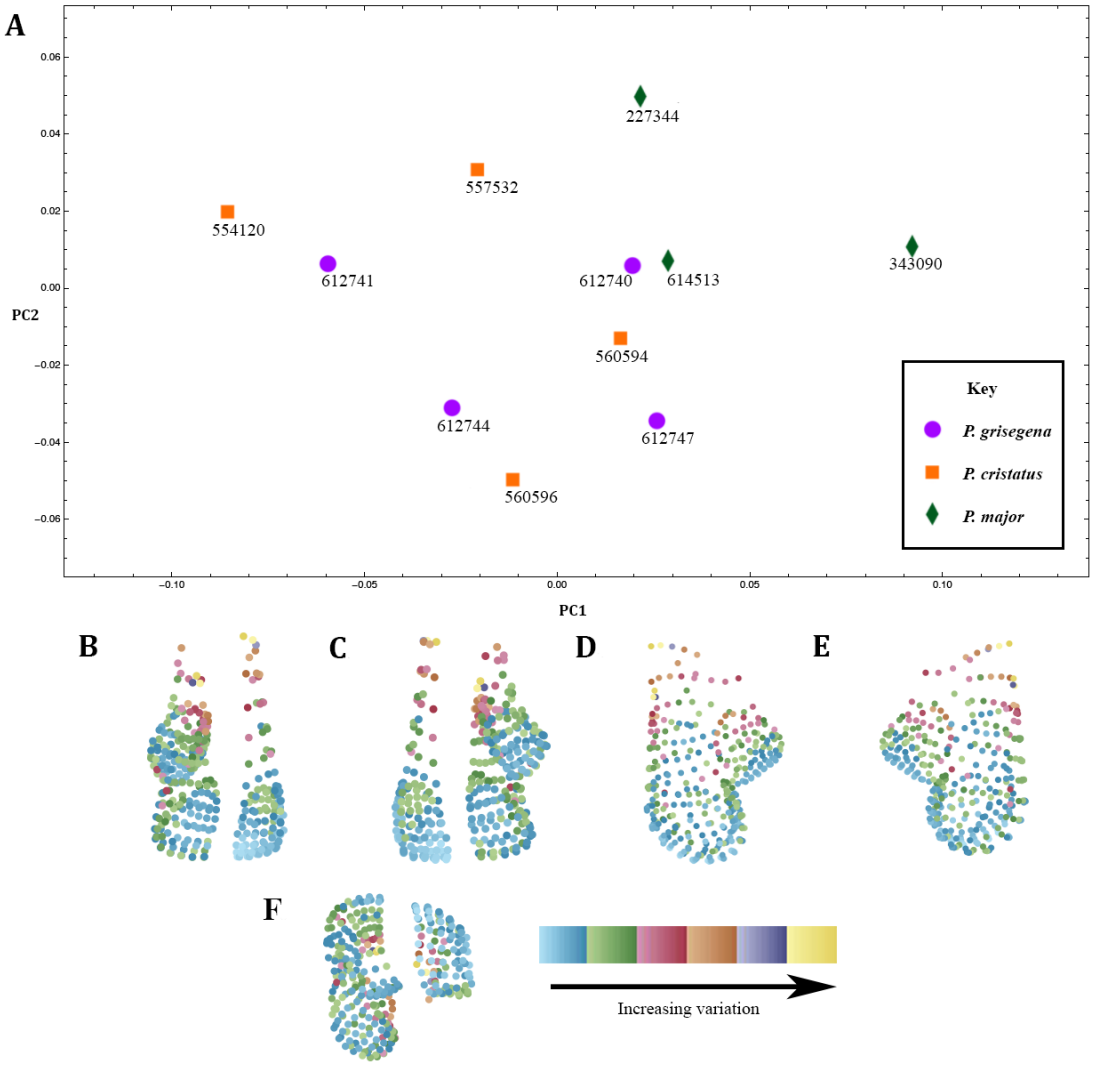

Figure 8: A) PC morphospace showing shape analysis for the distal tarsometatarsus of *Podiceps grisegena*, *P. cristatus*, and *P. major*. B) Dorsal view of variation map, C) ventral view, D) exterior view, E) interior view, F) distal view.

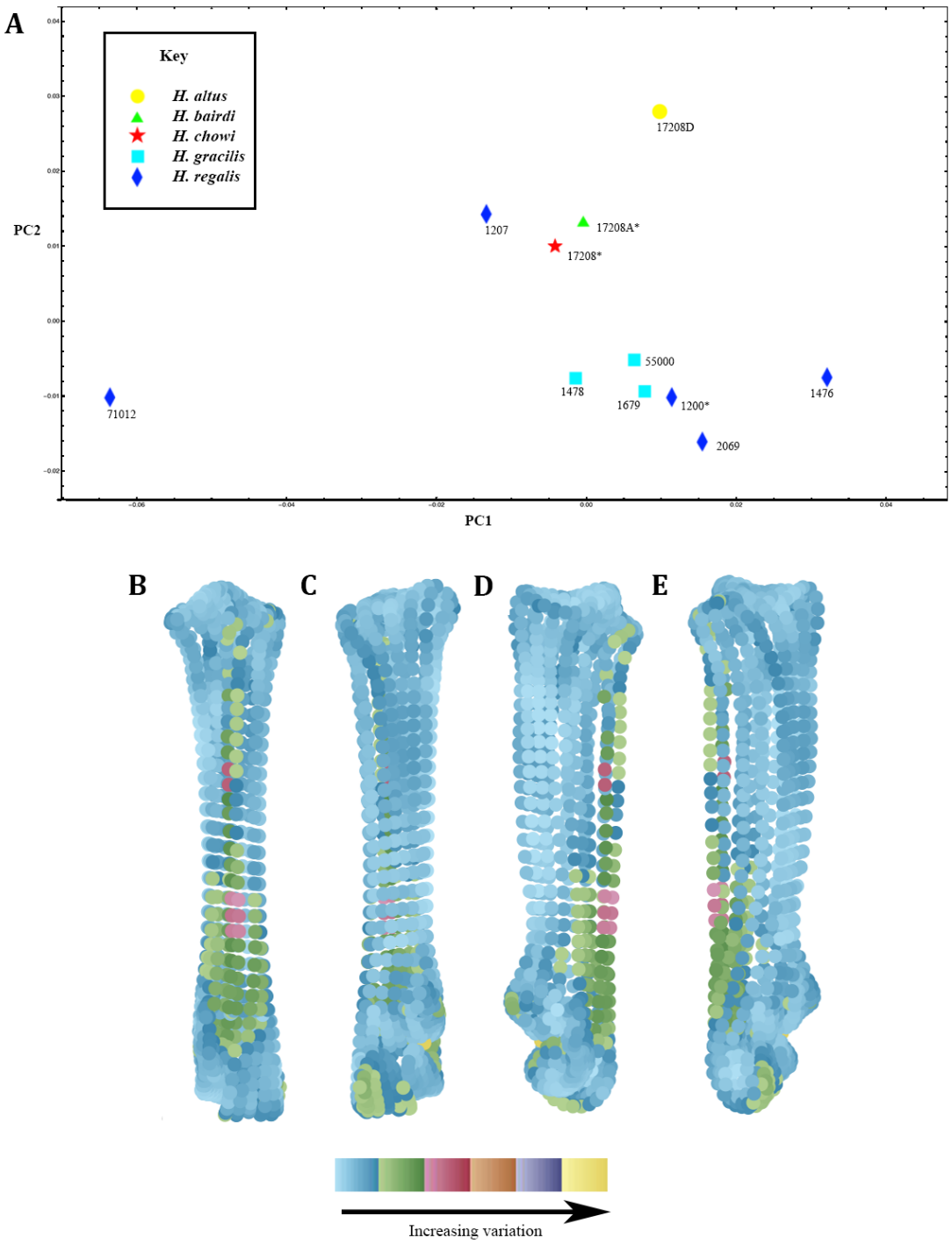

Figure 9: A) PC morphospace showing shape analysis for the full tarsometatarsus of *Hesperornis altus*, *H. bairdi*, and *H. chowi*, *H. gracilis*, *H. regalis*. B) Dorsal view of variation map, C) ventral view, D) exterior view, E) interior view. * represents type specimens.

Figure 10: *Hesperornis* specimens used for the full bone analysis PC2, showing breaks. Arrows point to breaks in the bone at very similar locations. Shape change occurs in this same area on the variation map. Specimens are lined up in order of shape change occurring along PC2, moving up the y-axis as images go from left to right. Specimens are not to scale.

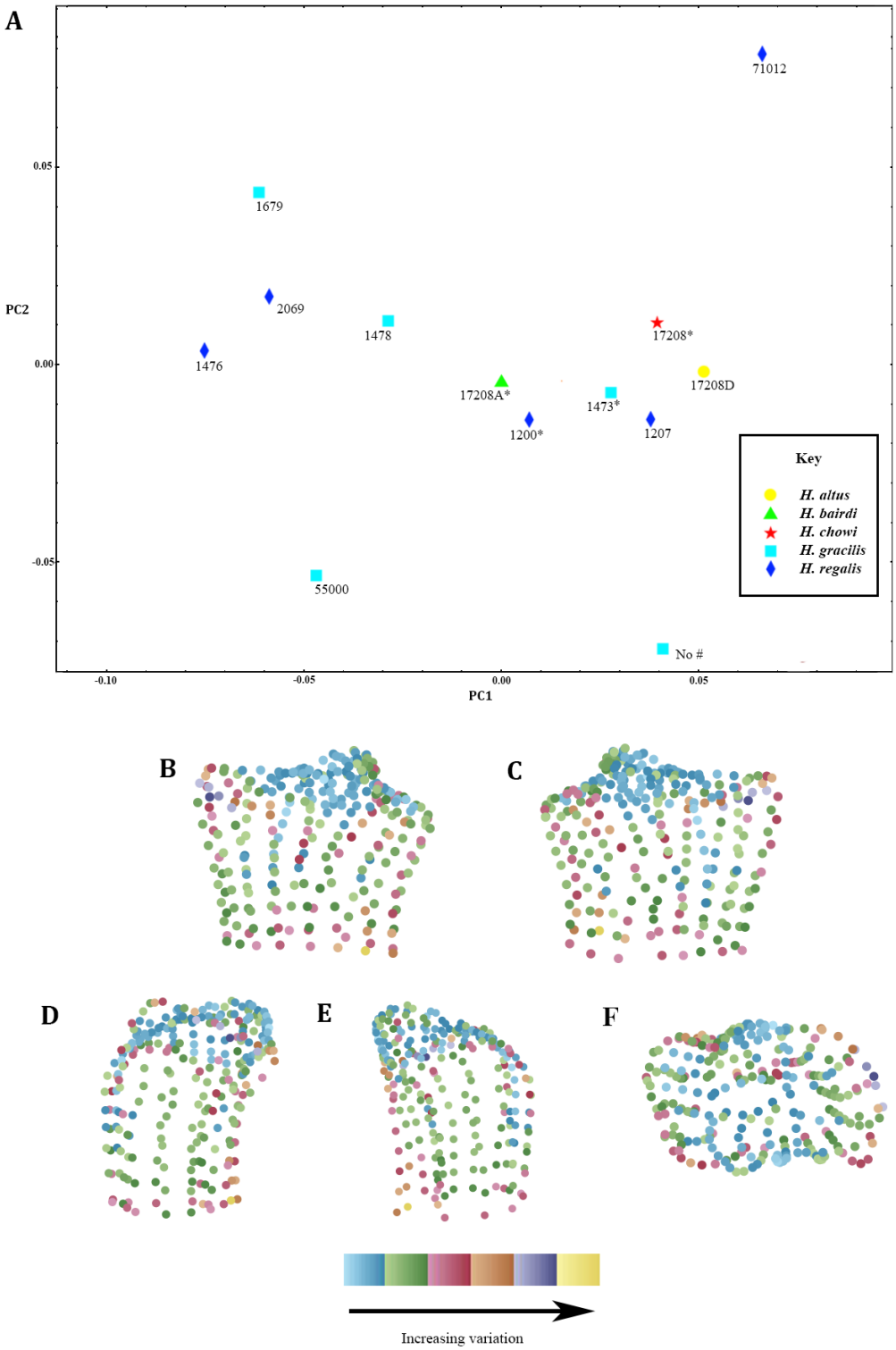

Figure 11: A) PC morphospace showing shape analysis for the proximal tarsometatarsus of *Hesperornis altus*, *H. bairdi*, *H. chowi*, *H. gracilis*, and *H. regalis*. B) Dorsal view of variation map, C) ventral view, D) exterior view, E) interior view, F) proximal view. * represents type specimens.

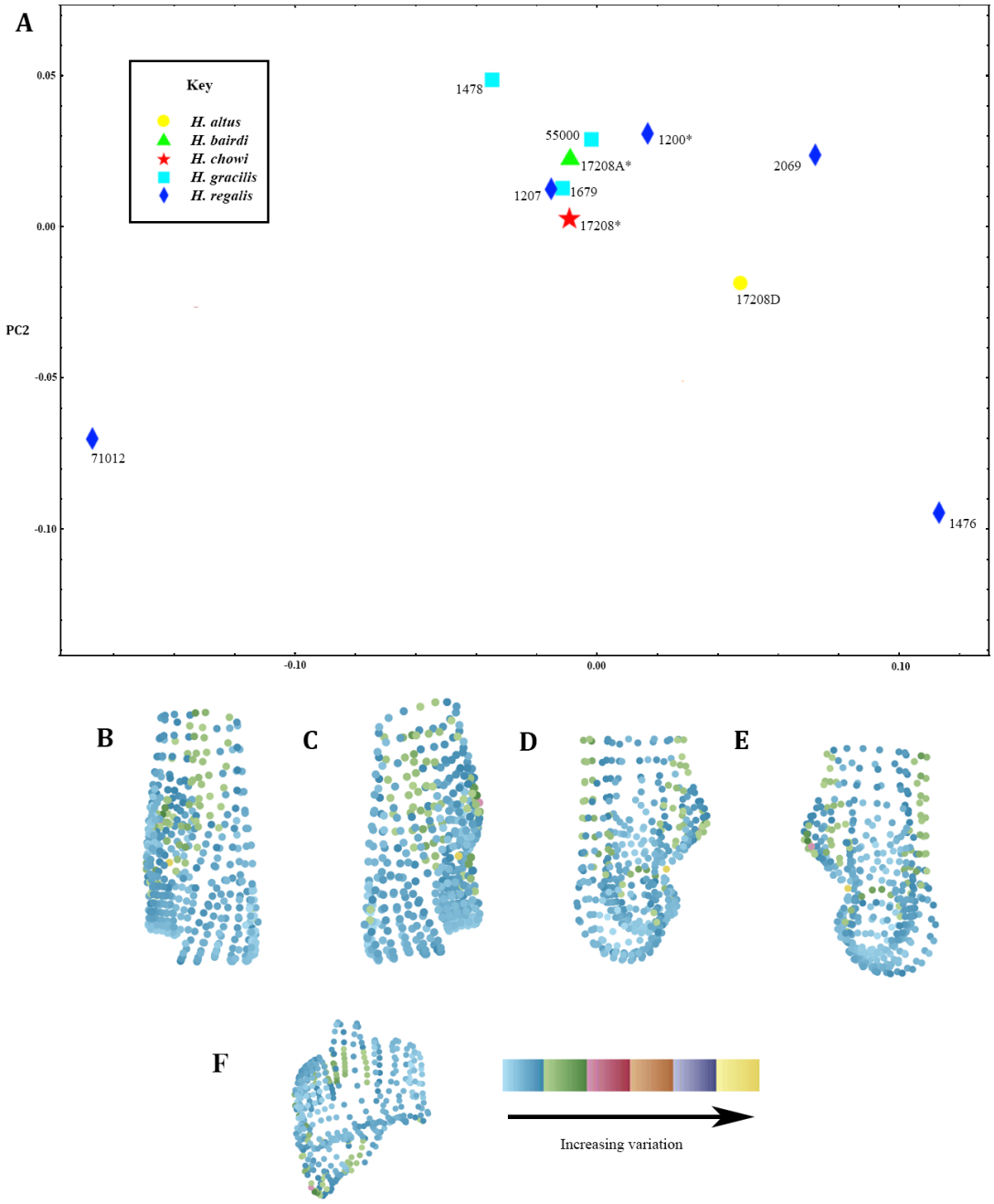

Figure 12: A) PC morphospace showing shape analysis for the distal tarsometatarsus of *Hesperornis altus*, *H. bairdi*, and *H. chowi*, *H. gracilis*, *H. regalis*. B) Dorsal view of variation map, C) ventral view, D) exterior view, E) interior view, F) distal view. * represents type specimens.